

Orientational anisotropy in oxygen dissociation on Rh(110)

Saw Wai Hla

*ICTP, Strada Costiera 11, I-34127 Trieste, Italy
and TASC-INFM Laboratory, Padriciano 99, I-34012 Trieste, Italy*

P. Lacovig

*TASC-INFM Laboratory, Padriciano 99, I-34012 Trieste, Italy
and Dipartimento di Fisica, Università di Trieste, via Valerio 2, I-34127 Trieste, Italy*

G. Comelli*

*TASC-INFM Laboratory, Padriciano 99, I-34012 Trieste, Italy;
Dipartimento di Fisica, Università di Trieste, via Valerio 2, I-34127 Trieste, Italy;
and Sincrotrone Trieste S.C.p.A., S.S. 14 Km. 163.5 in Area Science Park, I-34012 Basovizza-Trieste, Italy*

A. Baraldi and M. Kiskinova

Sincrotrone Trieste S.C.p.A., S.S. 14 Km. 163.5 in Area Science Park, I-34012 Basovizza-Trieste, Italy

R. Rosei

*TASC-INFM Laboratory, Padriciano 99, I-34012 Trieste, Italy;
Dipartimento di Fisica, Università di Trieste, via Valerio 2, I-34127 Trieste, Italy;
and Sincrotrone Trieste S.C.p.A., S.S. 14 Km. 163.5 in Area Science Park, I-34012 Basovizza-Trieste, Italy*

(Received 17 March 1999)

Scanning tunneling microscopy study of O₂ dissociation on Rh(110) at 170 K shows a low-energy dissociation coordinate for a precursor with the O-O axis aligned in the [001] azimuth, indicating a strong influence of the surface anisotropy on the potential-energy surface. This results in pairs of oxygen atoms oriented along [001], which aggregate in chains along $[1\bar{1}0]$. The atomic distance in the pairs, 3.3 Å, is shorter than the [001] lattice constant, which led to the conclusion that the oxygen sits in adjacent asymmetric short bridge sites and that the creation of ‘‘hot’’ oxygen atoms is not favored. [S0163-1829(99)15335-9]

Dissociative adsorption of O₂ on Rh(110) occurs at temperatures above 100 K and leads to a variety of ordered phases.¹ At low temperature, the only ordered phase is the saturation $(2\times 1)p2mg$ on the unreconstructed surface, whereas several ordered structures form on $(1\times n)$ reconstructed Rh(110) at temperatures above 480 K. A distinctive feature is that in all ordered structures oxygen is zigzag arranged in threefold sites along the $[1\bar{1}0]$ Rh rows. Oxygen adsorption on Rh(110) at low coverage and low temperature is poorly characterized. For oxygen coverage below 0.35 ML, when no long-range ordered structure forms, the vibrational² and photoemission³ studies ruled out occupations of threefold sites. The suggested long-bridge adsorption site is questioned in the recent theoretical calculations since this site does not show a minimum for the chemisorption energy.⁴ In the present paper we show that in the low-coverage regime the O/Rh(110) system is rather peculiar. On one side the atoms, created after dissociation at 170 K, remain as pairs, which seems to be rather common for low-temperature O₂ dissociation on metal surfaces.^{5,6} On the other hand, in contrast to the previously reported pairing of oxygen on the similarly corrugated Cu(110) surface, oxygen pairs on Rh(110) show very strong orientational ordering, short interpair separation, which decreases with coverage, and a tendency of the pairs to aggregate in long $[1\bar{1}0]$ chains, which establish a short-range ordered domain with 2×3 or $c(2\times 6)$ local structure in denser layers.

The experiment has been performed in an ultrahigh-vacuum system which hosts an Omicron variable temperature scanning tunneling microscopy (STM) instrument together with facilities for sample preparation and characterization. The Rh(110) sample was cleaned by repeated cycles of sputtering and annealing combined with treatments in oxygen and hydrogen ambient, until a sharp (1×1) low-energy electron-diffraction pattern was obtained. The STM images were recorded at the adsorption temperature, measured by means of a silicon diode attached on the back of the sample holder. The bias voltage applied to the W tip was varied within the ± 0.3 -V range and the images were collected in a constant current mode of 1 nA. For evaluation of the oxygen coverage, we used two different approaches, which gave the same results within 0.02 ML. The first procedure is counting the number of oxygen-related structures and normalizing to the atomic density of the (110) plane. The second procedure used the coverage versus exposure uptake for the same system reported in Ref. 3. For calibration of the exposure scale, we used the exposures yielding the sharpest $(2\times 2)p2mg$ pattern at 570 K, corresponding to 0.5 ML.

Figure 1 shows STM images for oxygen coverage of 0.26 ML [(a) and (b)] and 0.05 ML (c), respectively. In Figs. 1(a) and 1(b) the oxygen atoms appear as protrusions on the Rh surface, which is imaged as a sequence of parallel stripes corresponding to the $[1\bar{1}0]$ rows. The height of the protrusions is about 0.2–0.3 Å. The identification of the protrusions is about 0.2–0.3 Å. The identification of the protrusions is about 0.2–0.3 Å. The identification of the protrusions is about 0.2–0.3 Å.

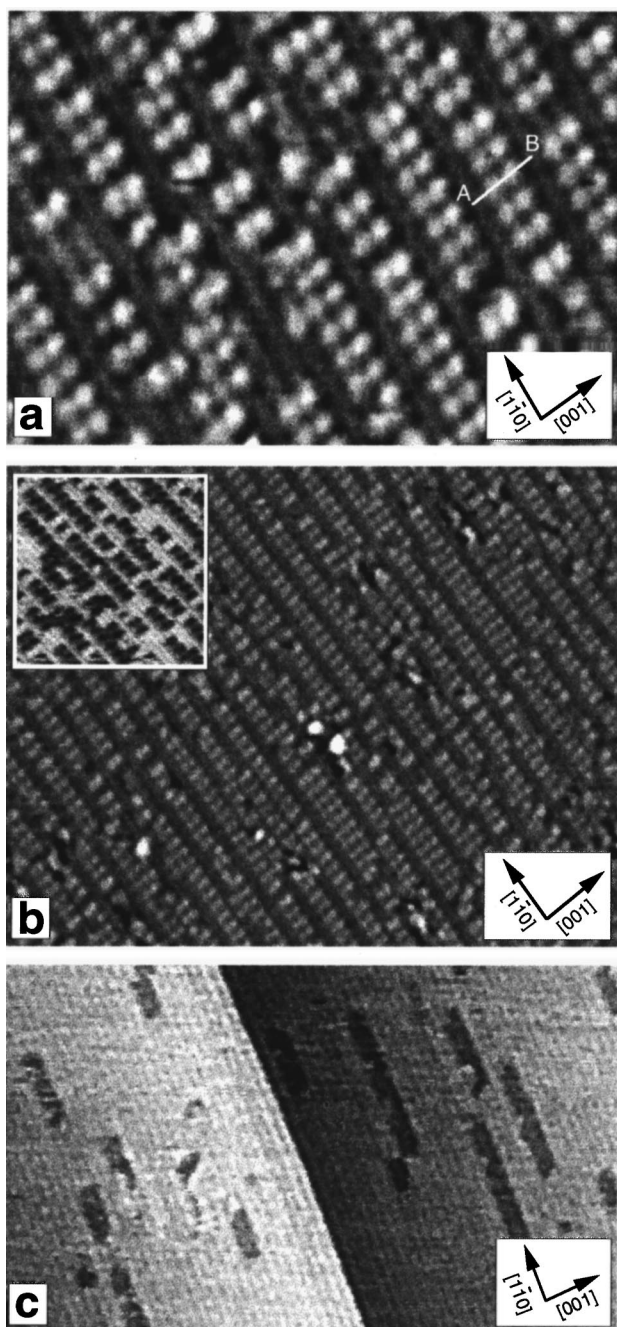


FIG. 1. STM images of the Rh(110) surface after different oxygen doses at 170 K. (a) 0.5 L, $110 \times 80 \text{ \AA}^2$, bias: -0.1 V , current: 1 nA ; (b) 0.5 L, $265 \times 210 \text{ \AA}^2$, bias: -0.1 V , current: 1 nA (inset: $105 \times 105 \text{ \AA}^2$, “black” oxygen, bias: -0.1 V , current: 1 nA); (c) 0.1 L, $290 \times 170 \text{ \AA}^2$, bias: -0.05 V , current: 1 nA .

sions as oxygen atoms is supported by the fact that in some images [inset in Fig. 1(b)] these protrusions are substituted by depressions, in accordance with other STM studies of oxygen adsorption.⁷ The appearance of the oxygen-related features strongly depended on the state of the tunneling tip, which in some cases unpredictably changed during scanning, resulting in conversion of the protrusions in depressions. As is clearly seen, the dominating oxygen-related features are close-spaced pairs of oxygen atoms aligned along the [001] direction, with each atom approximately aligned with the

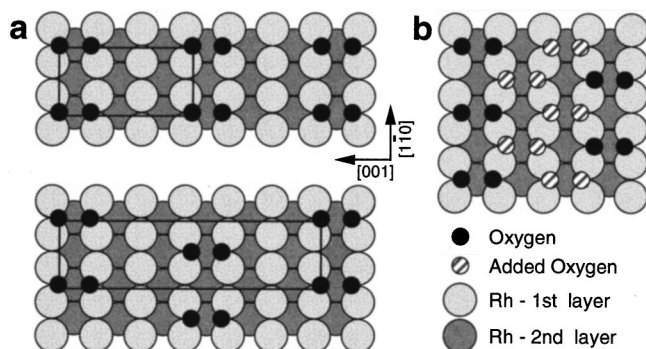


FIG. 2. Models of the (2×3) and $c(2 \times 6)$ (a) and “hexagon” (b) structures formed by the oxygen pairs on the Rh(110) surface.

underlying Rh $[1\bar{1}0]$ row. The resolution of the Rh atoms in the $[1\bar{1}0]$ rows is not sufficient to identify unambiguously the exact coordination of oxygen, but as discussed below, a short bridge adsorption site is the most likely. The pairs aggregate in chains along the $[1\bar{1}0]$ direction, with lengths up to 120 \AA . The distance between the pairs in the chains is $5.4\text{--}5.5 \text{ \AA}$, i.e., two $[1\bar{1}0]$ lattice constants.

The anisotropic orientation of the oxygen pairs and their aggregation in chains is an exclusive feature of the O/Rh(110) system. It occurs even at a very low oxygen coverage, as manifested by the image in Fig. 1(c), where chains containing from a few to more than ten pairs occur at 0.05 ML.

Figure 1 shows that the separation between neighboring chains depends on the oxygen coverage. At low coverage, the chains grow randomly separated by several O-free Rh rows. With increasing coverage, the separation decreases reaching the minimum distance of one O-free Rh row, as is apparent in Figs. 1(a) and 1(b). This results in a local (2×3) structure, when the pairs of the adjacent chains are aligned in phase, or a $c(2 \times 6)$ structure, when the pairs are out of phase [see the models in Fig. 2(a)]. It is clear though that many defects are present, leaving only a local order that cannot sustain a long-range-ordered structure.

Besides the pairs, triplets and a few single features can be seen as well, which make part of the defects in the local ordering. The triplets appear at coverages above $\sim 0.2 \text{ ML}$. Analysis of the atomic distribution with time has shown that the pairs are not mobile at this coverage, whereas the “third” atom in the triplets is rather mobile and hops attaching randomly to other pairs.

Figure 3 shows as data points the scan profile along the oxygen pair indicated by the line A-B in Fig. 1(a). The abscissa is calibrated against the distance between the O-free Rh rows, which give the secondary weak maxima separated by three [001] lattice constants, i.e., 11.4 \AA . The measured profile was fitted with two Gaussians of the same width. The free parameters in the fit were the Gaussian intensities, the distance between them, and their common width. The best fit is shown as a solid line. Applying the fitting procedure to several randomly selected pairs in different images, we obtained the average O-O distance, which is plotted as a function of coverage in the inset of Fig. 3. Despite the rather large error bars, which are partly due to the intrinsic static disorder of the structure, we observe a clear trend of a reduc-

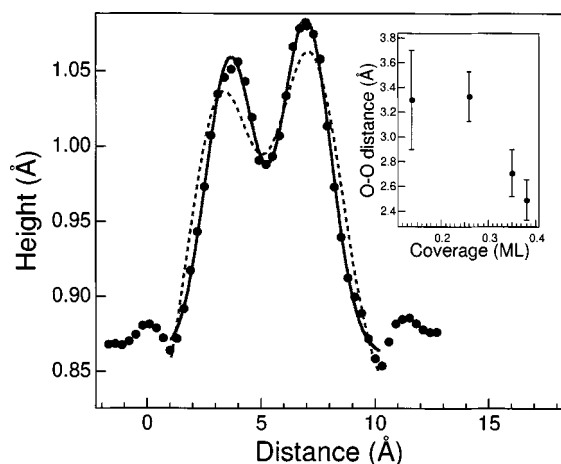


FIG. 3. *A-B* line scan of the image in Fig. 1(a) (data points), best fit (solid line) and fit with two Gaussians fixed at 3.8 Å (dashed line). The inset shows the O-O distance within the oxygen pairs as a function of the oxygen coverage.

tion of the O-O distance with oxygen coverage, from 3.3 ± 0.4 Å at the lowest examined coverage to 2.5 ± 0.2 Å at the highest one. Evidently the separation is smaller than the distance of 3.8 Å expected for oxygen adsorbed in short-bridge or on-top sites of the Rh $[1\bar{1}0]$ rows. In order to rule out a possible error due to the fitting procedure, we tried to fit the profile with two Gaussians at a distance of 3.8 Å, leaving all other parameters free. The resulting dashed curve in Fig. 3 is clearly inconsistent with the data. It is known that care has to be taken in interpreting the STM images as direct topographic maps of the surface.⁸ Nevertheless, as we consistently obtain this reduction in the O-O distance regardless of the scanning parameters used, and even from the images where the pairs appear as depressions, we conclude that the oxygen atoms are placed slightly asymmetrically, sliding towards the threefold sites. Most recently, *ab initio* calculations and the Tersoff-Hamann model have confirmed the correspondence between the position of the oxygen atoms and the protrusions in the STM images. This theoretical study has shown that a couple of oxygen atoms positioned in the symmetric short-bridge site appear in the image as two protrusions at a distance of exactly 3.8 Å.⁹

The present STM results are an example of a system with a very strong effect of the substrate surface anisotropy on the potential-energy surface for dissociation and negligible “ballistic” motion of oxygen atoms. The interpair separation for O₂ dissociation on Pt(111) and Cu(110) is usually more than one lattice constant, contrary to what should be expected considering the high diffusion barriers.^{5,6} This was explained in terms of nonthermal, transient motion due to partial transformation of the released adsorption energy into kinetic energy, which creates so-called “hot” atoms. The initial momentum of the oxygen atoms after dissociation makes them travel in opposite directions so that they can be found at distances as far as three lattice constants. For a similarly corrugated Cu(110) surface, the pairs were oriented either in $[1\bar{1}0]$ or $[001]$,⁵ with most probable separation of two lattice constants. This was interpreted in the framework of a molecular precursor model, suggesting that the pairs preserve the orientation of the oxygen molecules prior to dissociation.

The feature that distinguishes the O/Rh(110) system from O/Cu(110) and O/Pt(111) is that all pairs have the same orientation and the same (less than one $[001]$ lattice constant) interatomic separation. The orientation of the pairs indicates that the O-O axis of the molecular precursor before dissociation is aligned in the $[001]$ direction. A hollow site for the molecular precursor is the most likely one, as has already been evidenced for O₂ on Cu(110), but on that surface it did not show a preferential alignment in the $[001]$ or $[1\bar{1}0]$ azimuth.⁵ In contrast, the potential-energy surface of O₂ dissociation on Rh(110) is highly spatially anisotropic at low coverage, with a low barrier dissociation coordinate along $[001]$. Upon seizure of the O-O bond, the two atoms repel at a short distance and remain as a pair, preserving the $[001]$ orientation of the precursor. A $[1\bar{1}0]$ orientation of the molecular precursor cannot be excluded only for denser layers, where the separation between the chains is reduced and the repulsion prohibits the $[001]$ orientation. The third very mobile atom in the appearing “triplets” might be created by dissociation of a $[1\bar{1}0]$ precursor. The observed drastic reduction in the sticking coefficient at 0.25–0.35 ML can be related to this $[1\bar{1}0]$ precursor orientation less favorable for dissociation.³

For Rh(110), the diffusion barrier for oxygen (10–20 % of the oxygen adsorption energy⁶) should lie between 0.4 and 0.8 eV,¹⁰ comparable with that for Pt(111). Such diffusion barrier limits the atomic thermal motion of oxygen at 170 K to very short distances and only transient nondiffusive motion after dissociation of O₂ can cause the separations observed on Pt(111) and Cu(110) larger than ~ 4 Å.^{5,6} In contrast to Cu(110) and Pt(111), the interatomic separation of less than one $[001]$ lattice constant questions the creation of “hot” oxygen on the Rh(110) surface. This means that the chemical energy released during dissociative adsorption is very effectively dissipated to the phonon bath of the Rh substrate. The strong directional anisotropy of the dissociation coordinate can also be attributed to a reasonable traveling distance and weak repulsive O-O interactions provided by neighboring sites in the $[001]$ azimuth.

The exact location of the oxygen atoms cannot be directly deduced from the images, but the long-bridge site can be ruled out, because the pairs sit approximately on top of two adjacent Rh rows. Since the vibrational data² suggest either twofold or threefold oxygen coordination, the on-top site seems the least possible one in accordance with the recent theoretical study.⁴ The evaluated interatomic distance of ~ 3.3 Å suggests an asymmetric short-bridge site with atoms in the pair pointing towards the adjacent fcc threefold sites. Further shortening of the O-O distance in denser layers precedes the transition to the ordered $(2 \times 1)p2mg$ phase, where the atoms are in threefold sites, separated by 2.93 Å.¹¹ This finding clearly shows that simple classification of the adsorption sites as a short bridge, a long bridge, etc., is only an approximation. In reality, the adspecies are not rigidly trapped in the highest symmetric geometry and can undergo lateral movements responding to the charge-density changes induced by the interadsorbate interactions. It is interesting to note that in the rhodium oxide, Rh₂O₃, the O-O distance covers a remarkably similar range from 2.62 ± 0.09 to 3.14 ± 0.05 Å.¹²

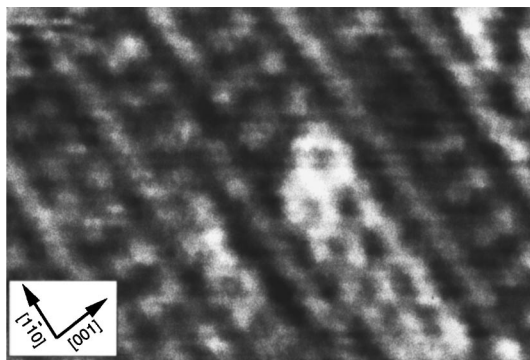


FIG. 4. $60 \times 40 \text{ \AA}^2$ STM image of the Rh(110) surface after 0.75-L oxygen dose at 170 K; bias: +0.07 V, current: 1 nA.

An interesting question is the mass transport involved in the aggregation of the pairs and formation of the $[1\bar{1}0]$ chains. Our results point to a mechanism with anisotropic diffusion barriers, which restrict the mobility to the $[001]$ direction. If we assume random dissociation, this would require that the pairs are very mobile and diffuse as units along the $[1\bar{1}0]$ direction until trapped at the most favorable distance of two lattice constants. As this appears to be very unlikely, we propose instead a scenario where a mobile molecular precursor is trapped in the $[1\bar{1}0]$ troughs and experiences a higher dissociation probability hitting existing oxygen pairs, resulting in the formation of long chains even at very low coverage.

The local (2×3) or $c(2 \times 6)$ “ordering” of the chains at higher coverages is evidently imposed by the compression of the adlayer. In this event, the chains behave as individual units; they grow randomly and the minimum allowed distance between the pairs of the adjacent chains is two $[001]$

lattice constants. The almost equal number of patches with in- and out-of-phase adjacent chains comes from the random growth, determined by the location of the first pair, which acts as a nucleation center. The maximum coverage corresponding to a perfect (2×3) or $c(2 \times 6)$ structure is 0.33 ML, not attained with the present only local order.

The transition state to the formation of the $(2 \times 1)p2mg$ islands is clearly manifested in Fig. 4. As is evidenced by the image, some oxygen pairs accommodate in the empty space between the chains, generating a layer that locally has a honeycomb structure [see the hexagons in the lower part of Fig. 4 and the model in Fig. 2(b)]. This structure, which is not stable on a large scale, can be regarded as a sequence of antiphase zigzag and zagzig oxygen chains decorating adjacent $[1\bar{1}0]$ Rh rows. Phase change of the zagzig oxygen chains naturally leads to the $(2 \times 1)p2mg$ structure. A strong interchain correlation of the zigzag O along the $[1\bar{1}0]$ direction has already been found by a He diffraction study.¹³

In conclusion, the Rh(110) surface exhibits three distinct properties for O_2 dissociation at low coverage different from the other previously studied transition metals. These are (i) a low-energy reaction path for the molecular precursor with an axis oriented in $[001]$; (ii) effective dissipation of the chemical energy released in the dissociative adsorption process, which prevents the formation of “hot” oxygen atoms; and (iii) asymmetric short-bridge adsorption sites for the oxygen atoms of the created pairs. Evidence for lateral movements of the atoms in the pairs, preceding the conversion to the three-fold sites in a dense layer, was given as well.

We would like to thank S. Baroni for helpful discussions. Financial support from the MURST under the program “COFIN97” is acknowledged.

*Author to whom correspondence should be addressed.

¹For a review, see G. Comelli, V. R. Dhanak, M. Kiskinova, K. C. Prince, and R. Rosei, Surf. Sci. Rep. **32**, 165 (1998).

²D. Alfè, P. Rudolf, M. Kiskinova, and R. Rosei, Chem. Phys. Lett. **211**, 220 (1993).

³G. Comelli, A. Baraldi, S. Lizzit, D. Cocco, G. Paolucci, R. Rosei, and M. Kiskinova, Chem. Phys. Lett. **261**, 253 (1996).

⁴K. Stokbro and S. Baroni, Surf. Sci. **370**, 166 (1997).

⁵B. G. Brinner, M. Doering, H.-P. Rust, and A. M. Bradshaw, Phys. Rev. Lett. **78**, 1516 (1997).

⁶J. Wintterlin, R. Schuster, and G. Ertl, Phys. Rev. Lett. **77**, 123 (1996).

⁷J. R. Mercer, P. Finetti, F. M. Leisble, R. McGrath, V. R. Dha-

nak, A. Baraldi, K. C. Prince, and R. Rosei, Surf. Sci. **352**, 173 (1996).

⁸F. Besenbacher and I. Stensgaard, in *The Chemical Physics of Solid Surfaces*, edited by D. A. King and D. P. Woodruff (Elsevier, Amsterdam, 1994), Vol. 7, p. 573.

⁹G. Cipriani and S. Baroni (private communication).

¹⁰G. Comelli, V. R. Dhanak, M. Kiskinova, N. Pangher, G. Paolucci, K. C. Prince, and R. Rosei, Surf. Sci. **260**, 7 (1992).

¹¹M. Gierer, H. Over, G. Ertl, H. Wolgemuth, E. Schwarz, and K. Christmann, Surf. Sci. **297**, L73 (1993).

¹²J. M. D. Coey, Acta Crystallogr., Sect. B: Struct. Crystallogr. Cryst. Chem. **26**, 1876 (1970).

¹³K. Prince, A. Morgante, D. Cvetko and F. Tommasini, Surf. Sci. **297**, 235 (1993).